Fibers and Polymers 2019, Vol.20, No.8, 1631-1640
DOI 10.1007/s12221-019-7999-8

ISSN 1229-9197 (print version)
ISSN 1875-0052 (electronic version)

Preparation of Intumescent Flame Retardant Poly(butylene succinate) Using Urea Intercalated Kaolinite as Synergistic Agent

Lingling Gu[1,2], Sheng Zhang[1,2], Hongfei Li[1,2], Jun Sun[1,2], WuFei Tang[1,2], Liqian Zhao[1,2], and Xiaoyu Gu[1,2]*

[1]*Key Laboratory of Carbon Fiber and Functional Polymers, Ministry of Education, Beijing University of Chemical Technology, Beijing 100029, China*
[2]*Beijing Key Laboratory of Advanced Functional Polymer Composites, Beijing University of Chemical Technology, Beijing 100029, China*

(Received November 18, 2017; Revised March 16, 2019; Accepted March 24, 2019)

Abstract: Urea (U) was successfully intercalated into Kaolinite (Kaol) and the product K-U was introduced into poly(butylene succinate) (PBS)/intumescent flame retardants (IFR) by melt blending. The structure of K-U was characterized by X-ray diffraction (XRD) and Fourier transform infrared spectroscopy (FTIR). The flame retardancy, thermal degradation, and combustion behavior of PBS composites were characterized by limiting oxygen index (LOI), vertical burning test to get UL-94 rating, thermogravimetricanalysis (TGA), and cone calorimeter test (Cone). With the introduction of K-U and IFR into PBS, the LOI obviously increased from 21.9 % for neat PBS to 40.1 % for composite containing 20 wt% IFR/5 wt% K-U; PBS cannot pass any UL-94 rating but the composite passed UL-94 V-0 rating. Similarly, the peak heat release rate (PHRR) in cone test decreased from 576 kW/m^2 to 292 kW/m^2. SEM results showed the char of the composite became more compact and smooth.

Keywords: Kaolinite, Urea, Poly(butylene succinate), Flame retardant, Mechanical properties

Introduction

Nanocomposite is composed of polymer and nano-distributed organic/inorganic particles [1]. Compared to neat polymer or conventional microcomposite, its many properties, especially mechanics and thermal properties are significantly improved [2]. It is worth mentioning that many research found nanoclay would improve flame retardant in polymer/ intumescent flame retardant (IFR) system [3]. In other words, many modified clay exhibited synergistic flame retardant [4-6].

Kaolinite (kaol) is typical nano-layered clay with basal spacing of about 0.76 nm, consisting of alternative layers of Al-O tetrahedron and Si-O octahedronat at the ratio of 1:1. In the past years, we focused on modification of kaol [7-12] and its synergistic flame retardant in polymer. Modified kaols of different compositions and structures were designed and prepared. And their contribution on synergistic flame retardant was probed in detail. During combustion, the composite containing kaol and IFR will form a carbonation-silicate shield on the material surface, which will prohibit heat conduction, at the same time crystal water in kaol will be released to absorb heat, as a result the mass loss of the materials was slowed down [13]. Similar to other polar inorganic particles, kaol is inclined to form aggregation in nonpolar polymer [14]. In previous work we also found modified kaol by organic groups would distribute at smaller size. As the modified kaol was designed as a synergistic flame retardant in our work, organic groups containing N/P/S was first considered.

Poly(butylene succinate) (PBS) is a biodegradable polyester [15]. It can be synthesized from either petroleum resources or biological resources. Taking environment into consideration, PBS has drawn more and more attention to develop its application. Like other aliphatic polymer, PBS is also inflammable material accompanied by severe dripping products. Its LOI value is less than 22.0 [16]. Just like other polyester resin, the serious molten drop maybe most troublesome. Intumescent flame retardant (IFR) has been considered as an ideal selection for its low smoke, low toxicity, and no dripping during combustion. Forth more, some research found a little amount nano clay would play the role of synergistic flame retardant in polymer/IFR [17]. Wang *et al.* reported that organic montmorillonite (OMMT) exhibited efficient flame retardancy in PBS/IFR [18]. Kaol and many kinds of modified kaol have been used as synergistic flame retardant in PP [13], PA6 [19], and PLA [14]. However, the application of kaol in PBS/IFR composites has not been reported to the best of our knowledge.

According to some literatures, urea was intercalated into kaol by solution method. Kaol was introduced into saturated urea aqueous solution [20]. In this work, we tried a novel way to prepare intercalated products just by direct grinding at different times and heating temperatures. The structure of products obtained at different conditions were characterized by FTIR and XRD. The distribution of kaol in PBS/IFR was observed by SEM. Finally, its influence on the flame retardant and mechanical performance of PBS/IFR was probed in detail.

*Corresponding author: guxy@mail.buct.edu.cn

Experimental

Materials

Polybutylene succinate (PBS, weight-average molecular weight: 130,000, relative density (25 °C)=1.26, melt flow index=20 g/10 min) was obtained from Kaixili Plastic Materials Company (Guangdong, China). Ammonium polyphosphate (APP, degree of polymerization ≥ 1,000) was produced in Jin Ying Tai Chemical Co., Ltd. (Jinan, China). Melamine (MA) was obtained from Jin Tong Le Tai Chemical Product Co., Ltd. (Beijing, China). Kaolinite (mean particle size of 10 μm) was provided by Xing Yi Mineral Processing Plant (Shijiazhuang, China). Urea was gotten from Beijing Chemical Works (Being, China).

Preparation of Urea Intercalated Kaol (K-U)

Scheme 1 shows the possible intercalation process of urea into kaol. Firstly, Urea and kaol at weight ratio of 1:1 are physically mixed by grinding for 30 min. The mixture was heated at 90 °C for 48 h. Then the mixture was washed by ethanol for several times and then dried at 60 °C for 12 h. The final product was named as K-U.

Preparation of PBS Composites

The PBS composites were prepared by melt blending using a micro twin-screw extruder (Wuhan Rui Ming Plastics Machinery Co., Ltd.). The screw speed was 44 rpm and the temperature of apparatus from hopper to die was 175, 180, and 180 °C, respectively. Table 1 presents the formulations of PBS composite. IFR was composed of APP/MA at the mass ratio of 5:1.

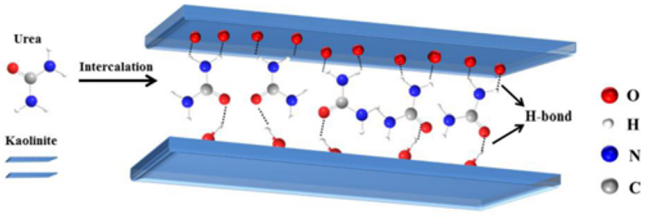

Scheme 1. Possible intercalation process of urea into kaol.

Table 1. Formulation of PBS composites

	PBS (wt%)	IFR (wt%)	Kaol (wt%)	K-U (wt%)
PBS	100			
PBS/IFR	75	25		
PBS/IFR/Kaol	75	24.5	0.5	
	75	23.5	1.5	
	75	22	3	
	75	20	5	
	75	18	7	
PBS/IFR/K-U	75	24.5		0.5
	75	23.5		1.5
	75	22		3
	75	20		5
	75	18		7

Measurements

Wide-angle X-ray diffraction (XRD) was carried out on a Rigaku D/max-2500 diffractometer with Cu-Kα radiation source (λ=0.154 nm). The interlayer spacing was calculated according to the following Bragg's equation (equation (1)).

$$n\lambda = 2d\sin\theta \quad (1)$$

where n is the order of reflection, d is the basal spacing, and θ is the diffraction angle.

Fourier transform infrared (FTIR) spectra were obtained by Thermo Nicolet Nexus 670 (USA) at the resolution of 1 cm^{-1} in 32 scans.

Thermogravimetric analysis (TGA) curves were recorded by using a TA Q-50 (USA) instrument under N_2 at the flow rate of 50 m*l*/min. The specimen (about 5 mg) was heated from room temperature to 800 °C at 10 °C/min.

Cone calorimeter test (CCT, Fire Technology Limited Co., Ltd.) was performed according to the standard ISO 5660 under a heat flux of 50 kW/m^2, the dimension of specimen was 100×100×3 mm^3, and they were wrapped in aluminum foil.

Limit oxygen index (LOI) was measured according to ISO 4589-2, the apparatus used is a JF-3 oxygen index meter (Jiangning Nanjing Analytical Instrument Co., Ltd., China). The sample dimension was 100×6.5×3 mm^3.

The vertical burning test was carried out on a CZF-3 apparatus (JiangningNanjing Analytical Instrument Co., Ltd., China) according to ISO 9773-1998 harmonized with UL-94 (Standard for Safety of Flammability of Plastic Materials for Parts in Devices and Appliances Testing). The sample dimension was 100×13×3 mm^3.

Morphological observation was performed by a Hitachi S-4700 (Japan) scanning electron microscopy (SEM) analysis at 20 kV acceleration voltage. All of the samples were coated with gold before measurement.

Raman spectra were obtained by a Renishaw inVia Raman microsope (USA) with the original wavelength of the laser was 633 nm at room temperature.

The mechanical tests were carried out on a CMT4104 tensile testing machine (SANS Company, China) according to ISO 527-1 standard. The samples were tested with a speed of 50 mm/min.

Results and Discussion

Characterization of K-U

Figure 1 shows the FTIR spectra of kaol, urea, and K-U. In the spectrum of kaol, those bands in 3620-3699 cm^{-1} are

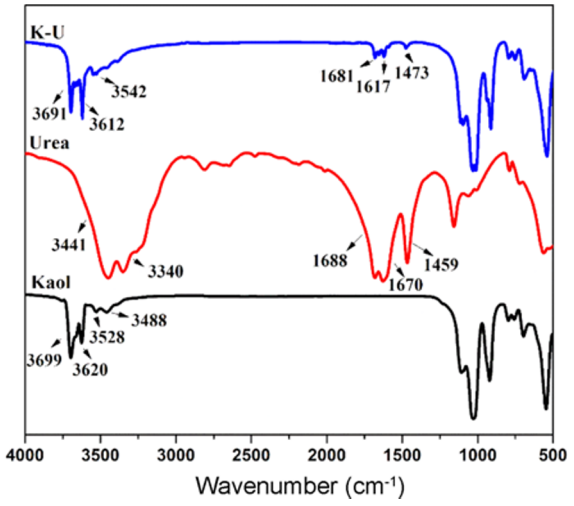

Figure 1. FTIR spectra of kaol, urea, and K-U.

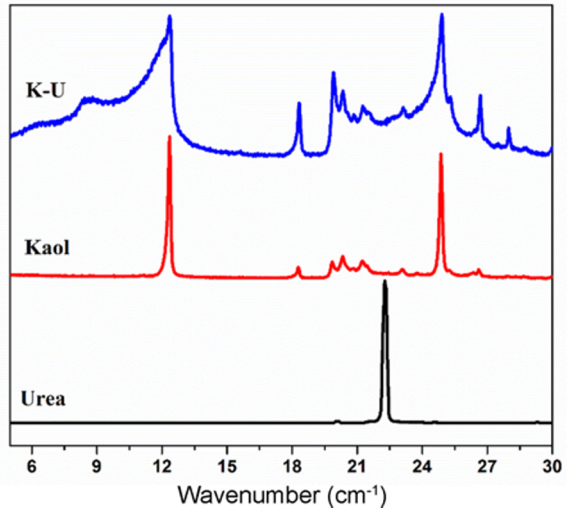

Figure 2. XRD patterns of urea, kaol, and K-U.

attributed to the hydroxyl stretching and bands around 1000 cm^{-1} are caused by Si-O vibration. In the spectrum of urea, special bonds appearing at 3441 and 3340 cm^{-1} are for $-NH_2$, 1688 cm^{-1} is for C=O and 1459 cm^{-1} for C-N. Almost all the bands of kaol and urea can be found in the spectrum of K-U, but with some position shift, indicating there existed some bonding between kaol and urea.

Figure 2 shows the XRD patterns of Urea, Kaol and K-U. For the urea, there was only one prominent peak at 2θ=22.3 °. For the raw kaol, the prominent peak at 2θ=12.3 ° of (001) crystal phase indicated its regular array, with interlayer spacing of 0.72 nm, whereas the peak was obviously widened and shifted to the left in K-U, indicating the layer order of raw kaol was disrupted. The lamellar spacing was enlarged and became random. A weak peak was formed around 2θ=8.2 °, corresponding to interlayer spacing about 1.08 nm. The enlargement is most possibly caused by the intercalation of urea.

Dispersion of Kaol/K-U and their Influence on Mechanical Performance

The distribution of kaol and K-U in PBS/IFR is investigated by SEM and shown in Figure 3. One can see from the fracture pictures that raw kaol was distributed as micron particle in composite, but K-U was distributed as nanoscale sheets. Combining with the XRD results above, for the lamellas were strutted in K-U, as a result it was inclined to be exfoliated after shear blend.

Generally, the introduction of inorganic particles into polymer matrix will bring obvious worsen on mechanical performance. The trend is also observed under the addition of flame retardant. In this work, both tensile strength and elongation at break of PBS were almost half dropped after the introduction of 25 wt% IFR. To face this problem, the inorganic particles are usually surface modified with some organic groups. According to the data listed in Figure 4 and

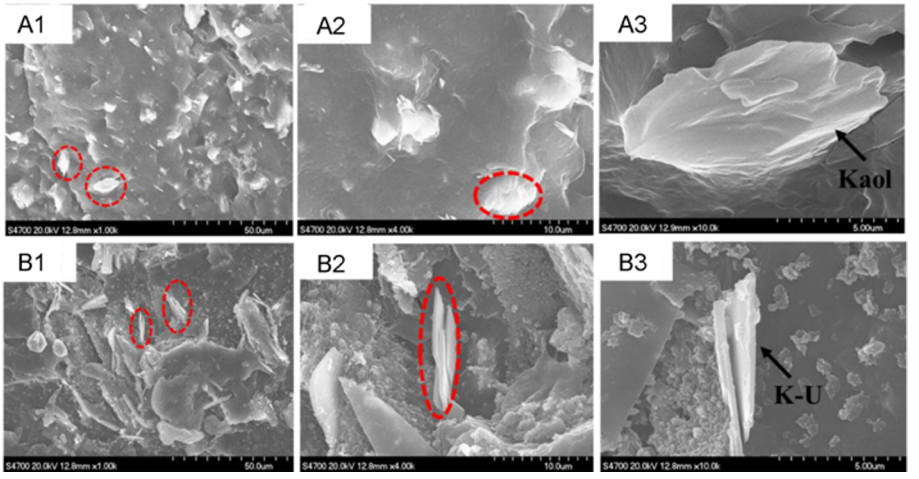

Figure 3. SEM image of PBS composites; (A1-A3) PBS/20IFR/5Kaol and (B1-B3) PBS/ 20IFR/5K-U.

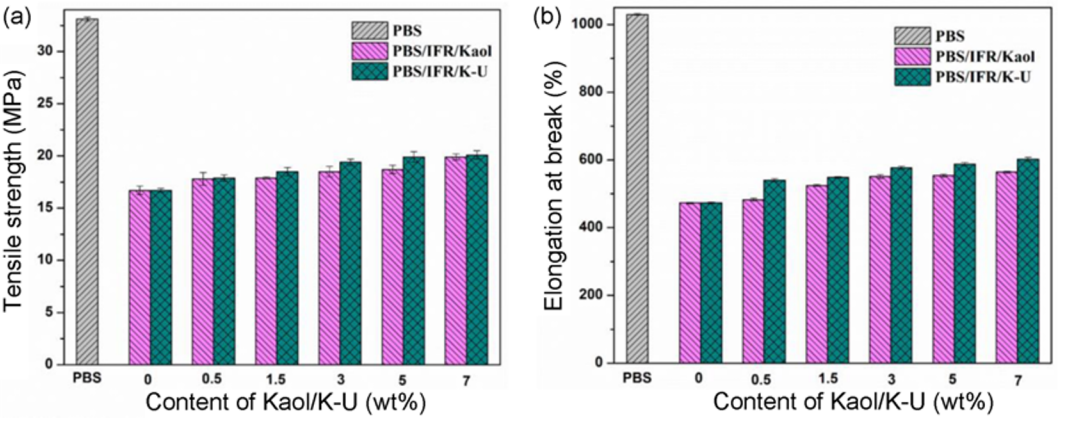

Figure 4. Tensile strength (a) and elongation at break (b) of PBS and its composites.

Table 2. Tensile strength and the elongation at break of PBS and its composites

Sample	Tensile strength (MPa)	Elongation at break (%)
PBS	33.1±0.1	1090±5
75PBS/20IFR	16.7±0.2	483±8
75PBS/20IFR/5Kaol	19.9±0.3	564±4
75PBS/20IFR/5K-U	20.1±0.2	602±6

Table 2, we found the worsened mechanical performance brought by IFR was somewhat restrained by K-U. The reason may be the urea to improve the interfacial force between IFR and PBS.

Based on many literatures, some nanoscale particles will form attraction with matrix. In other words, the phase interface compatibility and mechanical performance will be improved when the inorganic particles are dispersed at nanoscale in polymer. But aggregations of nano-particles often destroy this virtue. In this work, when the addition of K-U is less than 5 wt%, K-U will disperse in PBS as nanoscale sheet, as a result the worsening on mechanical properties brought by IFR was partly reduced.

Flammability

LOI and UL-94 Test

The LOI and UL-94 ratings of PBS composites are presented in Table 3. The LOI of neat PBS is only 21.9 % and it is burned with severe dripping. The melt dripping can remove the molten PBS matrix from the pyrolysis zone [21], but it can ignite the absorbent cotton and cannot pass any UL-94 rating. The introduction of 25 wt% of IFR raised LOI value to 31.7, but the molten drops cannot be controlled and UL-94 rating cannot be still passed. With increase in kaol/K-U content from 0.5 wt% to 1.5, 3, and 5 wt% by keeping the total addition at 25 wt% (at the same time IFR content was adjusted to 24.5, 23.5, 22, and 20 wt% accordingly), the

Table 3. LOI and UL-94 results of PBS and its composites

PBS and PBS composite	LOI (%)	UL-94		
		t_1/t_2	Dripping	Rating
PBS	21.9	5/>40	Yes	NR
75PBS/25IFR	31.7	11/0	Yes	NR
75PBS/24.5IFR/0.5 Kaol	34.3	4/0	Yes	V-0
75PBS/23.5IFR/1.5 Kaol	36.5	0/4	Yes	V-0
75PBS/22IFR/3 Kaol	37.4	0/1	No	V-0
75PBS/20IFR/5 Kaol	38.3	0/0	No	V-0
75PBS/18IFR/7 Kaol	36.9	0/1	Yes	V-2
75PBS/24.5 IFR/0.5 K-U	35.2	0/1	No	V-0
75PBS/23.5 IFR/1.5 K-U	38.9	0/0	No	V-0
75PBS/22 IFR/3 K-U	38.3	0/0	No	V-0
75PBS/20 IFR/5 K-U	40.1	1/3	No	V-0
75PBS/18 IFR/7 K-U	37.2	1/4	Yes	V-2

LOI of the composites also increased, the LOI reached the highest value of 40.1 in the presence of 5 wt% K-U, and all composites can pass the UL-94 V-0 rating. However, further increase of kaol/K-U content to 7 wt% resulted in decreasing LOI and UL-94 rating.

In the vertical burning test, a surprising phenomenon was that the serious dripping was effectively controlled at very low addition of K-U of 0.5 wt%.

Cone Calorimetry Test (CCT)

The CCT has been widely used to predict the burning behavior of materials under actual fire condition [22-28]. Several key data obtained in CCT such as heat release rate (HRR), peak of HRR (PHRR), and total heat release (THR) can be used to evaluate fire hazard.

HRR, THR, residual mass, and total smoke rate (TSR) curve results of PBS composites are shown in Figure 5 and relative some key data are presented in Table 4.

As shown in Figure 5(a) and (b), the combustion of neat PBS started 45 s after ignition and finished in 400 s with

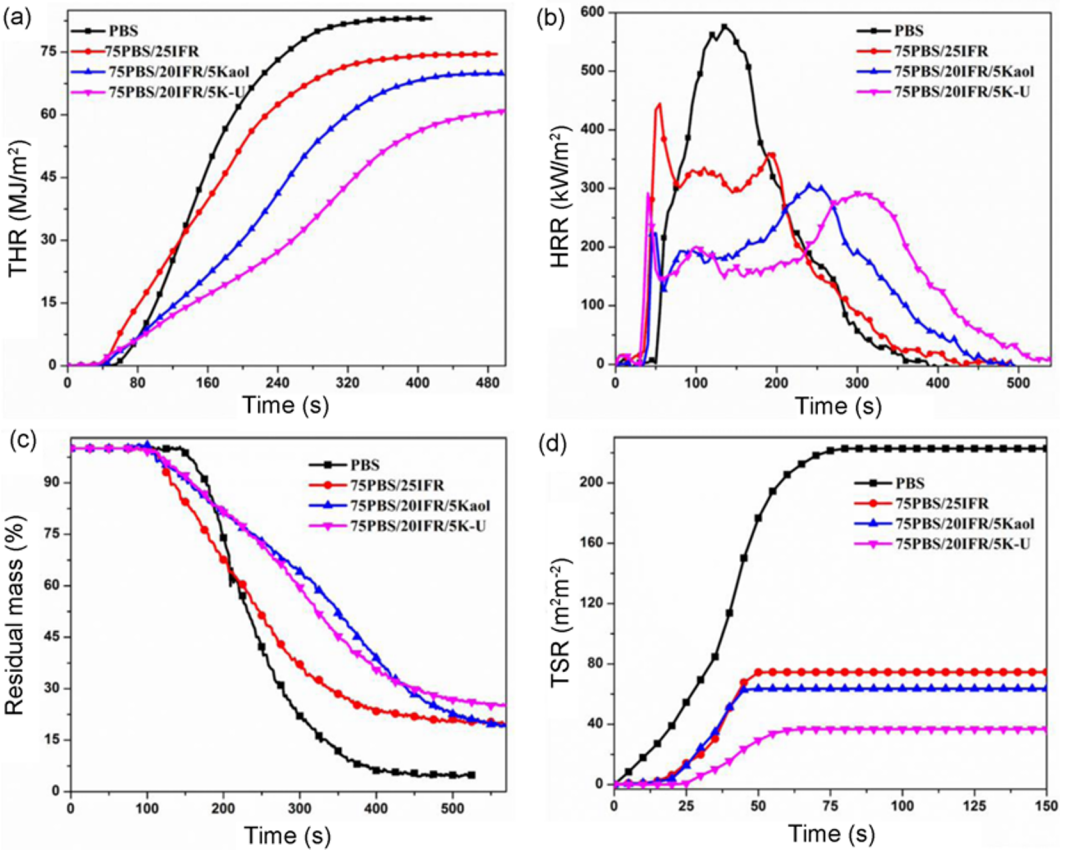

Figure 5. Heat release rate (HRR) (a), total heat release (THR) (b), mass loss (c), and total smoke rate (TSR) (d) curves for PBS and its composites.

Table 4. Key cone calorimeter data of PBS composites

Sample	TTI (s)	PHRR (kW/m^2)	AHRR (kW/m^2)	THR (MJ/m^2)	Residues (wt%)
PBS	45.2	576.3	283.3	83.5	5.0
75PBS/25IFR	27.4	445.5	287.7	74.2	20.8
75PBS/20IFR/5Kaol	33.6	305.1	172.3	70.4	26.3
75PBS/20IFR/5K-U	25.2	292.4	151.5	61.2	27.7

PHRR value of 576.3 kW/m^2 and THR of 83.5 MJ/m^2. The addition of 25 wt% IFR made the combustion happened earlier to 27 s after ignition, that was caused by early combustion of IFR, but PHRR was reduced to 445.5 kW/m^2 and THR decreased to 74.2 MJ/m^2. For 20 wt% IFR/5 wt% kaol (or K-U), the whole combustion time was prolonged over 500 s and PHRR was further reduced to 305.1 and 292.4 kW/m^2 and THR to 70.4 and 61.2 MJ/m^2.

Figure 5(c) shows the mass loss curves of PBS and its composites and the corresponding data are presented in Table 4. After burning, about 20.8 wt% char was left for neat 75PBS/25IFR, while the char increased to 26.3 wt% and 27.2 wt% for 75PBS/20IFR/5Kaol and 75PBS/20IFR/5K-U, respectively. In other words, the combination of IFR with Kaol/K-U promote the carbonization of PBS during combustion. Increased char residues mean decreased pyrolysis products and combustion heat release, which is in accordance with the PHRR behavior during cone calorimetry.

Figure 5(d) shows the total smoke rate (TSR) curves of PBS and its composites. Similar to other polyester, the combustion of PBS was accompanied by a large amount of smoke products. The smoke release was successfully restrained by the participation of IFR and the smoke was further hold down by kaol/K-U. The result may be associated with the more stable and compact char layer, which can prevent the escape of incomplete combustion products.

The results clearly documented the improvement from kaol, especially K-U to the flame retardant PBS/IFR

composites. The whole combustion process was prolonged and the heat release was controlled.

Char Analysis

Figure 6 shows digital photos of char residues of PBS and its composites after CCT. Little residue was left after combustion of neat PBS, whereas a relative coherent char layer was formed for PBS/IFR system, even though there existed some voids and the expansion height of the char residue was about 2 cm.

During combustion the char layer was impacted by the released gas. If the char layer become strengthened, it will generate less voids under the gas shock and the expansion height will be increased [29]. The expansion height increased to more than 3 or 4 cm for kaol or K-U adding respectively, indicating the char quality, including strength and density, were improved by the presence of stiff kaol/K-U [30]. The char morphology observed by SEM documented the change of char density. As shown in Figure 6, many holes were formed in the char of PBS/IFR, which may be due to the impact from the gas generated by the combustion of IFR [31], whereas smaller holes can be found in the char of PBS/IFR/Kaol and almost no obvious holes can be found in the char of PBS/IFR/K-U. The results showed the char quality was enhanced by the addition of kaol, especially K-U. The morphology can well interpret the heat release results obtained from CCT.

The char was further analyzed by Raman spectroscopy and the results was shown in Figure 7. There are two characteristic peaks in the Raman spectra, one is the D-band around 1431 cm^{-1}, corresponding to the defect peak, while the other at 1597 cm^{-1} called G-band, representing the graphite regularity. The intensity ratio of D-band to G-band ($I_{D/G}$), can represent the degree of graphitization. The smaller the value of $I_{D/G}$, the higher the degree of graphitization, indicating better quality of char.

It can be seen in Figure 7 that the intensities of both D and G-band increased significantly when 20 wt% IFR/5 wt% K-U were added. In general, the intensities of these two peaks was related to the degree of graphitization [32]. Calculated by the fitting area ratio, $I_{D/G,PBS}$ is 5.28, reduced to 2.21 for $I_{D/G,PBS/IFR/K\text{-}U}$, indicating the increase on graphite regularity. The results were consistent with char morphology observation.

It can be seen that the G bond was shifted to 1587 cm^{-1} from 1610 cm^{-1} (Figure 7(a)), generally the $\nu_{(C=C)}$ of G band in condensed ring molecules appeared around 1587 cm^{-1}. The down-shift of G band indicated the formation of carbon layer with pre-graphitization state after combustion.

Thermostability

The TGA and DTG curves under N_2 and air condition for

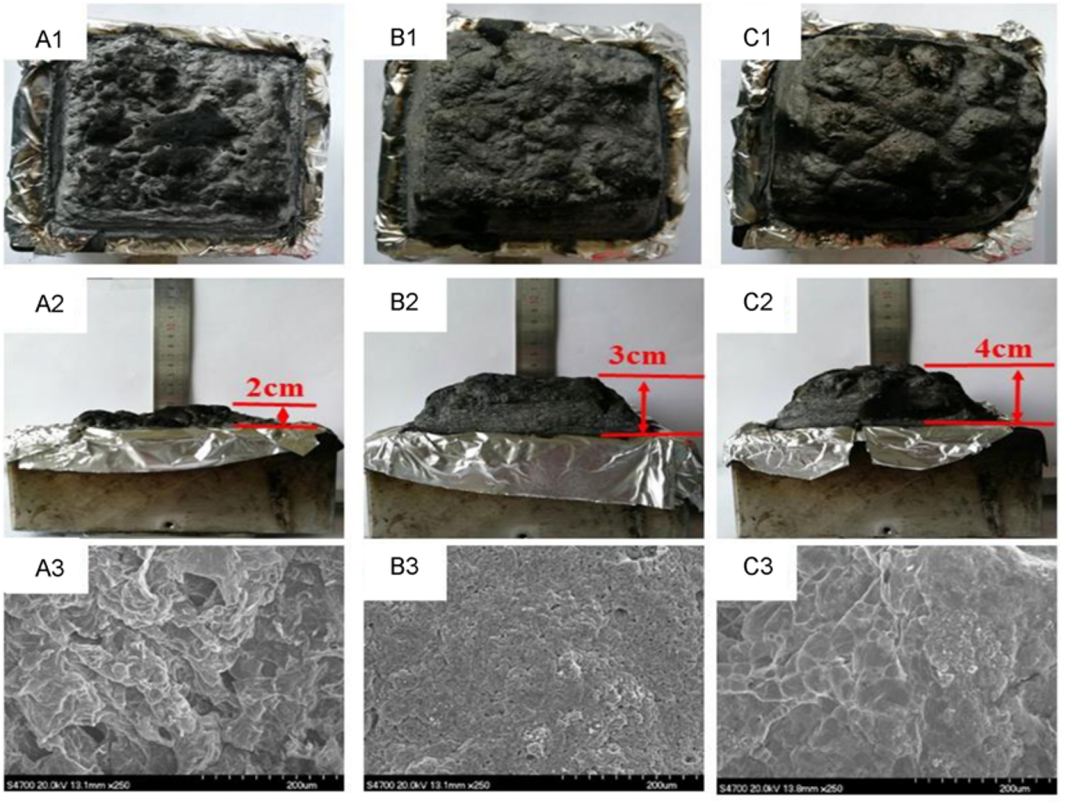

Figure 6. Surface (A1, B1, C1), profile (A2, B2, C2) and SEM (A3, B3, C3) photographs of char of PBS composites; (A) PBS/IFR, (B) PBS/IFR/Kaol, and (C) PBS/IFR/K-U.

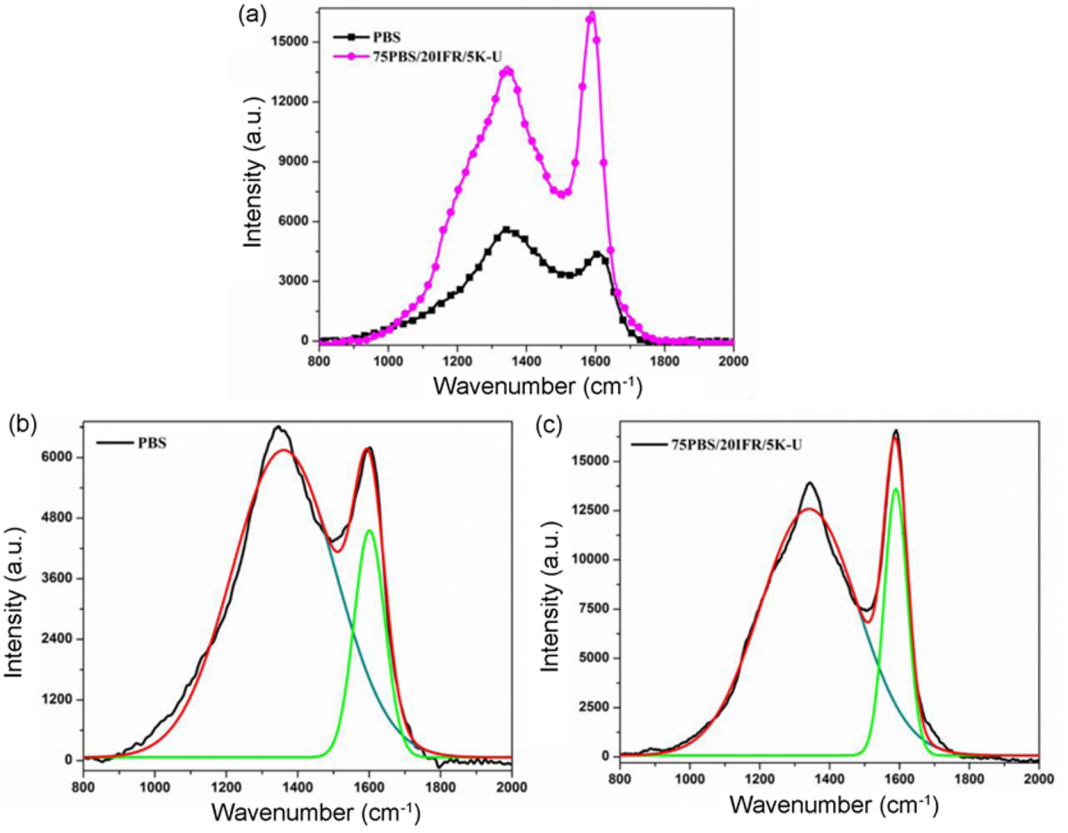

Figure 7. Raman spectra of the char residue for PBS and 75PBS/20IFR/5K-U after combustion (a), fitting results of PBS (b), and 75PBS/20IFR/5K-U (c).

neat PBS and its composites are presented in Figure 8 and the related data are shown in Table 5. PBS exhibited only one decomposition step during 340 to 420 °C both under N_2 and air condition, and almost no residue was left above 420 °C. By addition of IFR, the weight loss started from about 300 °C, earlier than neat PBS, which was caused by the decomposition of IFR [33,34]. The curves exhibited similar trend in N_2 and air, although key value of decomposition temperature and char content are a little different. As shown by the data in Figure 5, for the same sample, the decomposition was prolonged to relative higher temperature in air, but reduced char was left at high temperature. The results indicated O_2 in air would react with sample during heating.

The contribution of kaol/K-U on thermostability reflected in TGA is similar to the results in CCT. All the results documented both kaol and K-U can improve thermostability of PBS composites whether during heating or burning.

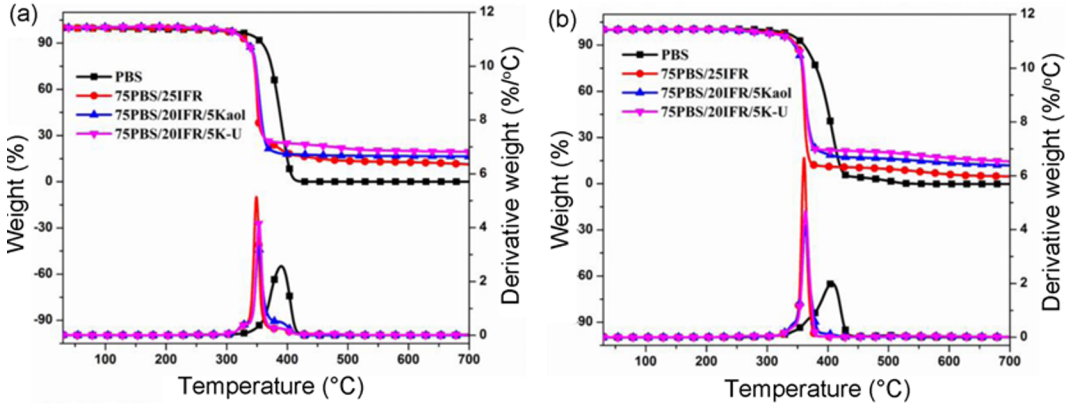

Figure 8. TGA and DTG curves of PBS composites under N_2 (a) and air (b) atmosphere.

Table 5. Key data of TGA curves for PBS composites under N_2 and air atmosphere

Sample	$T_{5\%}$ (°C)		$T_{50\%}$ (°C)		Residues at 700 °C (wt%)	
	N_2	Air	N_2	Air	N_2	Air
PBS	341.5	346.9	386.6	399.2	0	0
75PBS/25IFR	321.4	336.4	351.2	361.0	11.9	4.8
75PBS/20IFR/5Kaol	321.7	332.1	359.5	364.7	16.4	11.9
75PBS/20IFR/5K-U	320.4	331.9	355.6	364.5	19.5	12.5

Based on CCT and TGA results above, K-U gave the best contribution to heat release control during combustion and thermostability improvement during heating. The composition change at different heating temperatures was further reflected by FTIR. According to the data listed in Table 5, $T_{5\%}$ and $T_{50\%}$ is 320 and 355°C, respectively, and the whole decomposition finished until 700 °C. The photographs and FTIR spectra around these temperatures were collected in Figure 9.

At 320 °C, the appearance of the sample changed little and most special bonds were kept in FTIR, for example, bands (>3400 cm^{-1}) for the -OH of PBS; band around 1720 cm^{-1} for C=O, indicating the main skeleton of PBS was kept. When heating to 350 °C, about 50 wt% weight was lost, the sample was turned to black in color, and the intensity of the special bonds in FTIR spectra was weakened, but a series of new bonds were formed around 1000 cm^{-1}, which are special bonds for P=O and P-O-P. The new appearance and intensity change of IR absorption bands indicate the composition change, i.e, PBS has reacted with IFR/K-U and formed C/P/N complex, which was kept as char residue at higher temperature.

Flame Retardant Mechanism

The burning process and the possible decomposition and char formation scheme of PBS/IFR/K-U are presented in Figure 10. The general decomposition steps for PES/IFR during heat or combustion should be descripted as follow [35-40]: (1) APP decomposed and generated NH_3 and a large amount of phosphoric acid compounds such as $H_6P_4O_{13}$, $H_2P_2O_7$, H_3PO_4, and HPO_3. (2) Macromolecules of PBS degraded to units containing P-O-C structure, accompanied by the formation of conjugated polyenes. After continuous Diels-Alder reaction, the polycyclic aromatic hydrocarbons were finally formed. (3) With the increase of temperature, melamine gradually released NH_3, and generated melam, melem, and melon. These compounds tended to migrate upward under the gas flow. At the same time, kaol particles were also blown to the surface during combustion. At the presence of the stiff kaol particles, the char residue was strengthened [41,42]. (4) Urea was decomposed into NH_3 and HNCO at 150 °C, HNCO further oxidized and degraded to NH_3, NO/N_2O, and CO_2 [43]. Until the temperature increased above 270 °C, HNCO will further react with remaining urea to form MA. (5) Finally through the further cyclization reaction and bridging reaction, the condensed ring molecules gradually increased to form a pre-graphitization state of the carbon layer structure. (6) The aromatic structure will pack more closely

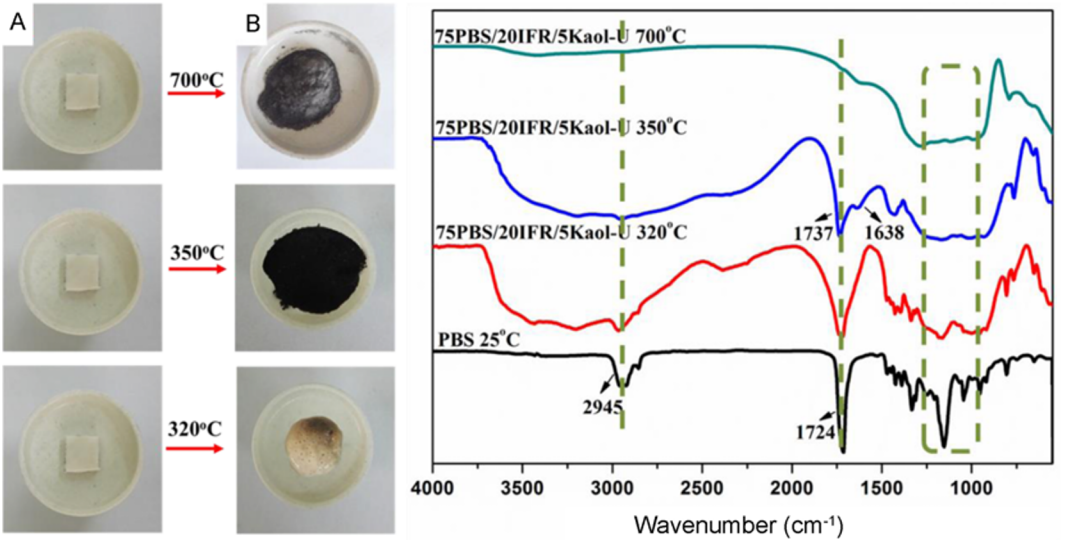

Figure 9. Digital photographs and FTIR spectra of PBS/IFR/K-U heated at different temperatures.

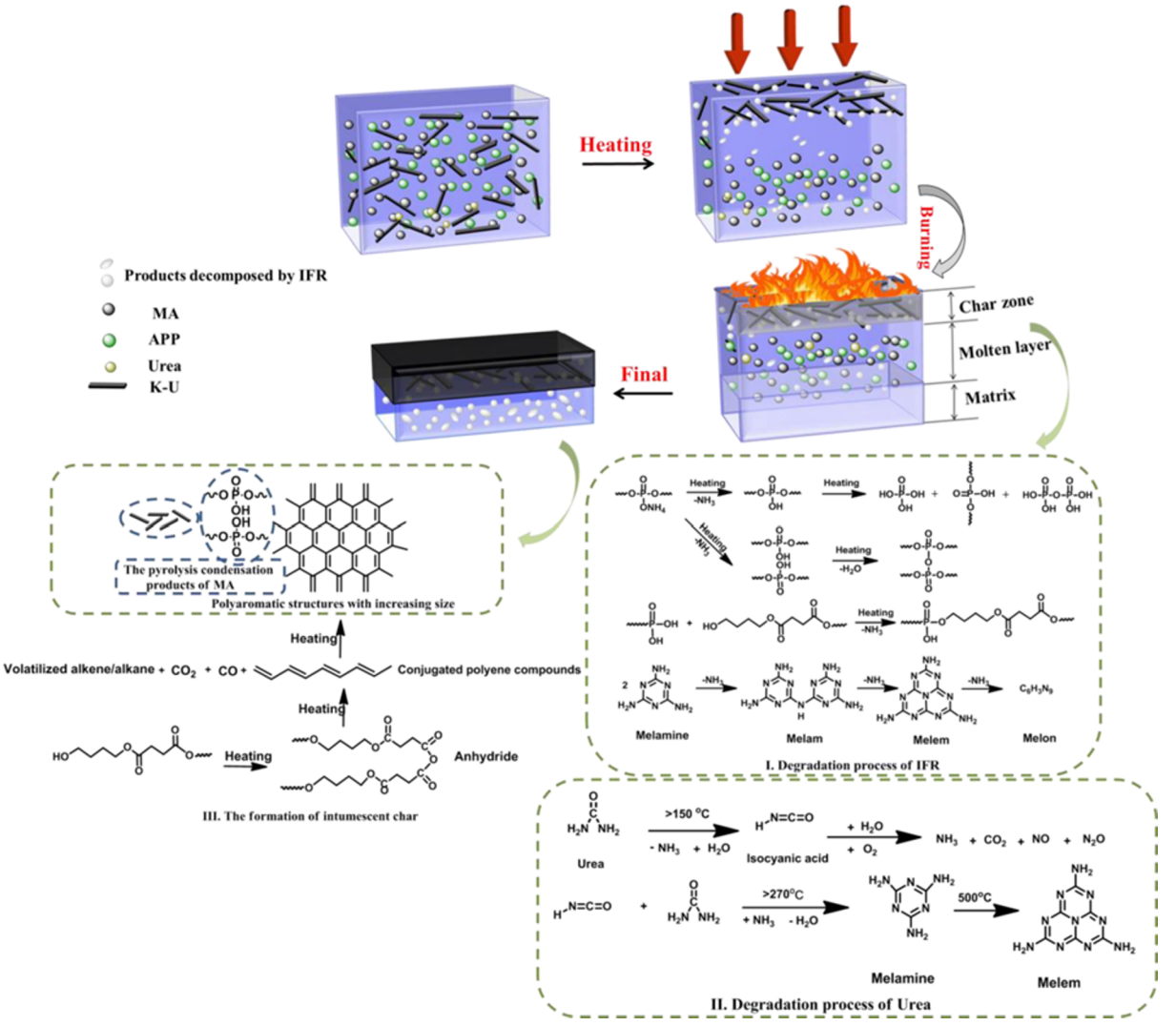

Figure 10. Possible flame retardant mechanism of PBS/IFR/K-U composites.

to form a graphite-like structure. (7) Water vapor, C/O oxide, and NH_3 generated during combustion promoted the formation of crosslinked residue. (8) At last the molten state was further expanded, gelled to form the char residue containing P/C/N.

The accumulation of kaol on the surface of the material can be used as a protective barrier, which limited the transfer of heat and oxygen to the material and reduced the volatilization of degradation products during combustion.

Conclusion

Urea intercalated kaol was prepared and used as synergistic flame retardant in PBS. In the composite of 75 wt% PBS/20 wt% IFR/5 wt% K-U, the LOI value reached 40.1 and obtained UL-94 V-0 rating, the severe dripping of PBS was thoroughly restrained by K-U. At the presence of K-U, the char layer formed after combustion became denser and smooth.

Acknowledgment

The authors would like to thank the National Natural Science Foundation of China (No. 21674008) for their financial support of this research.

References

1. Y. Zhang, C. Yu, P. Hu, W. Tong, F. Lv, P. K. Chu, and H. Wang, *Appl. Clay Sci.*, **23**, 632 (2012).
2. T. Gcwabaza, S. S. Raya, and A. Maity, *Eur. Polym. J.*, **45**, 353 (2009).
3. P. Zhao, S. Liu, K. Xiong, and Y. Liu, *Fiber. Polym.*, **17**, 569 (2016).

4. S. S. Ray, K. Okamoto, and M. Okamoto, *Macromolecules,* **36**, 2355 (2003).
5. P. Kiliaris and C. D. Papaspyrides, *Prog. Polym. Sci.,* **35**, 902 (2010).
6. G. R. Saad, H. F. Naguib, and S. A. Elmenyawy, *J. Therm. Anal. Calorim.,* **111**, 1409 (2013).
7. Y. Jiang, X. Gu, S. Zhang, W. Tang, and J. Zhao, *Mater. Lett.,* **150**, 31 (2015).
8. W. Tang, S. Zhang, J. Sun, H. Li, X. Liu, and X. Gu, *Thermochim. Acta,* **648**, 1 (2017).
9. W. Tang, S. Zhang, X. Gu, J. Sun, X. Jin, and H. Li, *Appl. Clay Sci.,* **132-133**, 579 (2016).
10. W. Tang, S. Zhang, J. Sun, and X. Gu, *Ind. Eng. Chem. Res.,* **55**, 7669 (2016).
11. W. Tang, J. Han, S. Zhang, J. Sun, H. Li, and X. Gu, *Polym. Compos*., **39**, 3461 (2018).
12. X. Hou, H. Li, and Q. Liu, *Appl. Surf. Sci.,* **347**, 439 (2015).
13. W. Tang, L. Song, S. Zhang, H. Li, J. Sun, and X. Gu, *J. Mater. Sci.,* **52**, 208 (2017).
14. R. D. Kambel, B. A. Aliyu, J. T. Barminas, and A. Akinterinwa, *Int. J. Mater. Chem.,* **7**, 14 (2017).
15. Y. Tachibana, T. Masuda, M. Funabashi, and M. Kunioka, *Biomacromolecules*, **11**, 2760 (2016).
16. L. Ferry, G. Dorez, A. Taguet, B. Otazaghin, and J. M. Lopez-Cuesta, *Polym. Degrad. Stab.,* **113**, 135 (2015).
17. W. Tang, X. Gu, Y. Jiang, J. Zhao, W. Ma, P. Jiang, and S. Zhang, *J. Appl. Polym. Sci.,* **132**, 14 (2015).
18. Y. Wang, S. Zhang, X. Wu, C. Lu, Y. Cai, L. Ma, G. Shi, and L. Yang, *J. Therm. Anal. Calorim.,* **128**, 1417 (2017).
19. J. Sun, X. Gu, M. Coquelle, S. Bourbigot, S. Duquesneet, M. Casetta, and S. Zhang, *Polym. Adv. Technol.,* **25**, 1552 (2014).
20. S. Zhang, Q. Liu, F. Gao, X. Li, C. Liu, H. Li, A. S. Boyd, C. T. Johnston, and B. J. Teppen, *J. Phys. Chem. C,* **121**, 402 (2016).
21. K. Fukushima, M. Murariu, G. Camino, and P. Dubois, *Polym. Degrad. Stab.,* **95**, 1063 (2010).
22. S. Yu, H. Xiang, J. Zhou, and M. Zhu, *Fiber. Polym.,* **18**, 1098 (2017).
23. X. Wang, Y. Hu, L. Song, H. Yang, B. Yu, B. Kandola, and D. Deli, *Thermochim. Acta,* **543**, 156 (2012).
24. P. Kiliaris and C. D. Papaspyrides, *Prog. Polym. Sci.,* **35**, 902 (2010).
25. J. Bian, L. Han, X. Wang, X. Wen, C. Han, S. Wang, and L. Dong, *J. Appl. Polym. Sci.,* **116**, 902 (2010).
26. B. Schartel and T. R. Hull, *Fire Mater.,* **31**, 327 (2007).
27. S. Chang, M. Nguyen, B. Condon, and J. Smith, *Fiber. Polym.,* **18**, 666 (2017).
28. T. Kashiwagi, Jr. RHH, X. Zhang, R. M. Briber, B. H. Cipriano, S. R. Raghavan, W. H. Awad, and J. R. Shields, *Polymer,* **45**, 881 (2004).
29. S. H. Jeong, K. H. Yoon, B. G. Min, Y. S. Lee, S. P. Lee, and S. B. Park, *Fiber. Polym.,* **18**, 1638 (2017).
30. Y. Tang, Y. Hu, S. Wang, Z. Gui, Z. Chen, and W. Fan, *Polym. Int.,* **52**, 1396 (2003).
31. G. R. Saad, H. F. Naguib, and S. A. Elmenyawy, *J. Therm. Anal. Calorim.,* **111**, 1409 (2013).
32. P. Lespade, R. Al-Jishi, and M. S. Dresselhaus, *Carbon,* **20**, 427 (1982).
33. Y. Liu, L. Mao, and H. Shu, *J. Appl. Polym. Sci.,* **131**, 8964 (2014).
34. S. Bourbigot, M. L. Bras, and R. Delobel, *Carbon,* **33**, 283 (1995).
35. S. Bourbigot and S. Duquesne, *J. Mater. Chem.,* **17**, 2283 (2007).
36. X. Zhang, X. Tang, R. Wang, R. Wang, X. Yan, and M. Shi, *Fiber. Polym*., **18**, 1421 (2017).
37. C. Hoffendahl, G. Fontaine, and S. Bourbigot, *Polym. Degrad. Stab.,* **98**, 1247 (2013).
38. C. Lu, X. Gao, D. Yang, Q. Cao, X. Huang, J. Liu, and Y. Zhang, *Polym. Degrad. Stab*., **107**, 10 (2014).
39. U. Braun and B. Schartel, *Macromol. Mater. Eng*., **293**, 206 (2008).
40. L. Yang, Y. Liu, C. Ma, Y. Wu, W. Liu, C. Zhang, F. Wang, and L. Li, *Fiber. Polym.,* **17**, 1018 (2016).
41. S. Pappalardo, P. Russo, D. Acierno, S. Rabe, and B. Schartel, *Eur. Polym. J.,* **76**, 196 (2016).
42. H. Chen, X. Wen, Y. Guan, J. Min, Y. Wen, H. Yang, X. Chen, Y. Li, X. Yang, and T. Tang, *Fire Mater.,* **40**, 1090 (2016).
43. M. Ayoub, M. F. Irfan, and K. S. Yoo, *Energy Convers. Manage.,* **52**, 3083 (2011).